

Review of Computer Engineering Research

2024 Vol. 11, No. 3, pp. 85-98

ISSN(e): 2410-9142

ISSN(p): 2412-4281


DOI: 10.18488/76.v11i3.3850

© 2024 Conscientia Beam. All Rights Reserved.



Detection and localization of wrist fractures in x-ray imagery using deep learning teaching

 Haider Abdulbaqi
Abbas Mohammed¹

 Shaymaa Taha
Ahmed²

 Rana Mohammed
Hassan Zaki³

 Qusay Kanaan
Kadhim⁺⁺

^{1,2,4}Department of Computer Science, University of Diyala, Baqubah 32001,
Iraq.

¹Email: haiderabdulbaqi@uodiyala.edu.iq

²Email: Shaimaa.Ahmed@uodiyala.edu.iq

³Email: dr.qusay.kanaan@uodiyala.edu.iq

³Department of Computer Science, University of Technology, Baghdad 00964,
Iraq.

³Email: rana.m.zaki@uotechnology.edu.iq



(+ Corresponding author)

ABSTRACT

Article History

Received: 13 December 2023

Revised: 29 April 2024

Accepted: 16 May 2024

Published: 6 August 2024

Keywords

Convolutional neural networks

Deep learning

Recurrent neural network

Transfer learning

Wrist fractures

X-ray images.

Hospitals often refer patients with wrist fractures, particularly to their emergency rooms. To accurately diagnose these illnesses and choose the appropriate course of therapy, doctors must evaluate images from various medical equipment, medical data, and a physical assessment of the patient. This project attempts to use deep learning on these images to identify wrist X-ray fractures and help physicians diagnose them, particularly in emergency departments. This study employs a dataset comprising both fractured and regular wrists to assess the extent to which the Recurrent Neural Network with 22 Convolutional Neural Network layers (RN22-CNNs) transfers knowledge for fracture identification and classification. We evaluate the diagnostic accuracy of the RN-21CNN model against four popular transfer learning models, namely Visual Geometry Group (Vgg16), ResNet-50, Inception V3, and Vgg19. We used the model on a dataset of 1644 X-rays collected from the Kaggle repository. Next, we trained, verified, and tested the adapted (RN22-CNNs) model. The proposed model had an accuracy of 96.61%. The proposed Computer-Aided Diagnosis System (CADS) will save medical practitioners' burden by accurately identifying fractures.

Contribution/Originality: This work aimed to develop a deep-learning model for fracture identification and classification. Various feature extraction approaches were used to identify the most critical features from the photos and the medical data.

1. INTRODUCTION

When we examine the areas where bone fractures occur, we frequently see fractures of the wrists, shoulders, and arms, among other body parts, especially in hospital emergency rooms [1]. Furthermore, observations reveal that fractures can manifest as complete or partial breaks in the bones, stemming from a diverse range of causes. This category includes both closed and open bone fractures [2]. A deep wound exposes the skin to an open fracture, also known as a complicated fracture [3]. A closed fracture, also known as a simple fracture, happens when the bone remains intact despite the skin breaking. It was found that placing more stress on the bone than it can withstand is the most frequent cause of fractures [4] after looking at the causes of bone fractures. Therefore, falls, trauma, or a direct blow to the body can cause bone fractures. Overuse or repetitive motions, which wear down the muscles and increase the strain on the bone, commonly cause stress fractures in athletes [5]. Diseases that weaken bones, such as osteoporosis or bone cancer, can also cause fractures. Unexpected pain, bruising, swelling, apparent deformity,

warmth, or redness can all result from bone fractures [6]. As part of the processes used to discover bone fractures, doctors may prescribe testing for fractures, in addition to a complete medical history that includes inquiries about the mechanism of the fracture and a physical examination. The X-ray, Magnetic Resonance Imaging (MRI), and Computerized Tomography (CT) are the three primary instruments used in these procedures [7]. The X-ray gadget, which is also more affordable than the alternatives, is the most favored of this equipment. In this study, deep learning based fracture diagnosis in wrist images was conducted using X-ray images that were received from Kaggle [8].

Since bone X-rays are quick and inexpensive to obtain, doctors rely on them for diagnosis, evaluation, and classification. To preserve the X-ray image of the bone, a machine applies a tiny quantity of ionizing radiation to a body part, such as the hand, foot, thigh, elbow, wrist, and other bony body parts [9]. Early and accurate diagnosis of bone abnormalities can prevent numerous detrimental effects for the patient. Due to their bulk, bones absorb a large amount of radiation, while soft organs allow some of the radiation to pass through. Photographic film captures the radiation efficiencies, making the soft organs and bones appear nearly white [10]. This film's nearly gray tint makes it feasible to see structural flaws and alterations in the bone in order to identify anomalies in the bone. In order to help doctors diagnose and treat a wide range of medical conditions, Hospitals and other healthcare facilities usually maintain X-ray images in their databases [11]. One of the main areas of image processing is edge detection. Since every image has a boundary or an edge. The plan is to research and evaluate different edge detection techniques in order to determine which is the most effective approach for edge detection in x-ray imaging. Techniques for processing images include feature extraction, edge detection, categorization, acquisition, and filtering [12]. Obtaining an x-ray of the bones is simple, but getting a precise diagnosis quickly enough to preserve the patient's life is more challenging. The application of machine learning and artificial intelligence has benefited both patients and specialists. One of the current issues in health centers is the untrained medical personnel and laymen viewing X-rays, which can lead to an incorrect diagnosis, as well as the specialist doctor taking a long time to prepare the medical report—up to 20 minutes or more—and the blurry X-ray images, which can make it challenging to extract features [13].

Deep learning approaches have drawn interest from researchers looking to enhance the accuracy of X-ray picture classification and diagnosis. Several of them fought to present models and techniques that would enable sophisticated diagnostics and yield categorization because of feature extraction and modeling, which uses several layers for data processing, followed by testing and dataset training. Following its introduction in the late 1990s, the convolutional neural network (CNN) gained enormous popularity, in comparison to other models, especially in the classification of images and the very accurate extraction of characteristics from them, as well as other two-dimensional data [14]. The goal of neural networks is to imitate the structure of the brain. They employ a network of interconnected "neurons" to gather, summarize, and/or transform input before sending the values to the next neuron in the sequence. This procedure results in an output layer, which we can use to provide predictions. It takes a ton of data to build and train a neural network from scratch. Numerous computer servers operating nonstop for weeks at a time enable the training of innovative image classification networks on millions of image data sets. Most medical researchers believe this to be impractical. Applying the technique of transfer learning. To train a new model for a particular task, this technique involves taking huge, pre-trained CNNs and utilizing their powerful, highly polished characteristics as a starting point, as shown in Figure 1.

In the clinical setting, transfer learning has not received much attention, despite the abundance of picture data available. Transfer learning from pre-trained CNNs can yield human-level diagnostic outcomes in the classification of skin lesions and the definition of disease on digital retinal images, as shown by [15]. However, recent research has published some encouraging results. Plain radiograph analysis has not yet demonstrated comparable levels of diagnostic accuracy. For instance, after retraining the GoogLeNet CNN for pathology detection in plain frontal chest radiographs, we obtained an area under the curve of between 0.861 and 0.964 for several chest radiograph features.

A different study used transfer learning from a pre-trained ImageNet CNN to automatically classify osteoarthritis in knee radiographs [15].

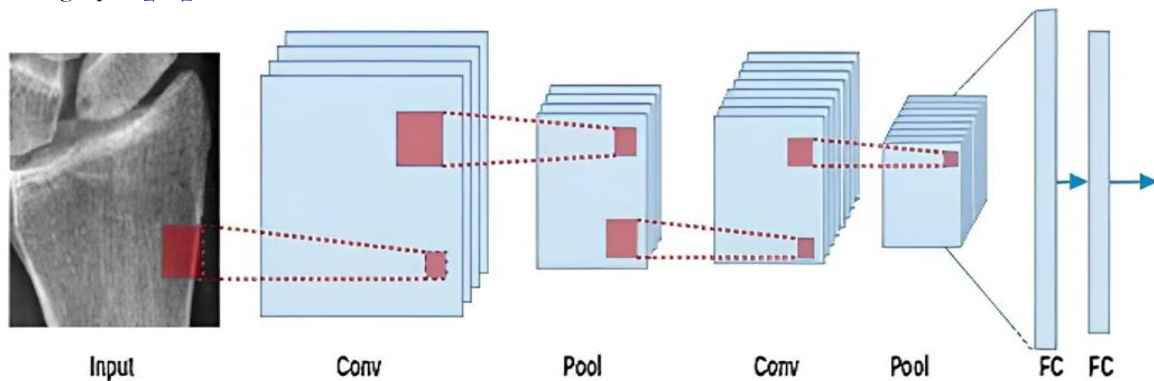


Figure 1. A single-channel input image is subjected to a CNN-based classifier.

Each convolutional layer (Conv) converts the input into a three-dimensional volume of activated neurons. In each feature map of its input volume, the pooling layer (Pool) independently and spatially samples the volume. Fully-Connected layers (FC) produce a prediction at the conclusion [16]. In the past, radiology's use of Computer-Aided Recognition (CAR) did not always result in increases in diagnostic accuracy, which reduced physician sensitivity and required unnecessary further diagnostic testing. There is a lot of excitement about the potential applications of deep learning approaches to CAR in medicine, but there is not much proof yet that these approaches can improve diagnosis accuracy in applications that are clinically important. In this work, we developed a 22-layer Convolution Neural Network (RN-22CNN) based on residual networks. This network was trained on a wrist fracture dataset with high-quality labels to produce an automated crack recognition system that could match the diagnostic accuracy of a team of orthopedic specialists. The majority of earlier studies think that residual networks are a good option for categorizing and indexing the features of the wrist images in the area. There are also some restrictions on the residual network that are noted. The difficulty of the layers spreading information from shallow layers to deeper layers increases with model depth, leading to information loss. To overcome this issue, researchers couple the residual network with a 22-layer CNN model [17].

The following are the primary contributions of this study, which uses deep-learning-based object detection models to conduct fracture detection on wrist X-ray images:

1. Using the RN-22CNN model, the burden on doctors is reduced by accurately classifying the crack locations in an X-ray picture.
2. The features needed to identify a wrist fracture can be extracted by the model. In the experiment, we show that our model can more accurately represent the wrist fracture.
3. In terms of accuracy, precision, recall, and f1-score, the RN-22CNN model outperformed the four well-known pre-trained classifiers and state-of-the-art classifiers, achieving the greatest classification accuracy of 96.61%.

This paper organizes the related works, methodology, data collection, feature extractors, RN-22CNN model, performance metrics, results, discussion, and conclusion.

2. RELATED WORKS

To generate precise results that can help decision-makers in hospitals and health facilities, the main focus has been on deep learning model training on a range of patient datasets. Many researchers have applied machine learning and artificial intelligence to the medical field, which has proven beneficial. Researchers have processed a variety of data, text, and image formats to provide reports that enhance the quality and efficacy of medical work for the diagnosis, classification, and prognosis of certain human diseases. The literature includes studies on artificial intelligence-based fracture diagnosis using open-source and clinical bone imaging datasets from various medical

devices. The work of [Esteva, et al. \[18\]](#) is categorized as "Object classification, localization, and detection," which refers to simultaneously determining an object's kind, location, and presence in an image. By using a The Graphics Processing Unit (GPU)-powered deep learning technique, the ImageNet Large-Scale Visual Recognition Challenge produced the first functional core in 2012, which brought together a number of researchers with the goal of developing and improving computer vision.

As a result, deep learning models were then put into practice, and they all yielded correct and successful outcomes, especially in the areas of diagnosis and medicine, where the models' classification and detection accuracy was on par with or occasionally better than that of a typical doctor's diagnosis. The Convolutional Neural Network (CNN), a type of deep learning algorithm that hardcodes translational invariance, an essential feature of image data, should receive the most recognition. It is capable of gathering similar photos and completing other tasks, as well as extracting differences and analyzing data from a substantial amount of data, thereby splitting jobs effectively. More research and the creation of diverse deep learning models are necessary to address the issues the medical industry faces.

[Cernazanu-Glavan and Holban \[19\]](#) trained a convolutional neural network with a set of medical images, such as X-rays and CT scans, of people with certain illnesses. The images had pooling, convolutional, and fully linked layers. The convolutional neural network first receives the images and flattens them into vectors. In the end, the likelihood is that the "elements" in the images stand in for the ability to identify the illness of the output vector," which is what the softmax layer ultimately stands for. During the training phase, we iteratively change the internal network layer parameters to increase accuracy. Lesser layers typically detect basic forms and edges in images, which influence higher-level representations, aiming to answer questions such as "Is there a disease or not?" based on the typical or abnormal training outputs.

After testing the algorithm on a dataset of 433 images, [Esteva, et al. \[20\]](#) found that using CNN and Gastrointestinal Stromal Tumor (GIST) features produced the best results, with an accuracy rate of 0.87–0.94 for the various pathologies. This study "looks into how well CNN learned from a non-medical dataset can spot different kinds of pathologies in chest X-rays and rates the effectiveness of deep learning methods for finding pathologies in chest radiographs." The results, which are based on non-medical learning, demonstrate the effectiveness of deep learning algorithms in detecting pathology in chest X-rays.

A classification model for "periapical examination regions based on periodontal bone destruction" was introduced by [Moran, et al. \[21\]](#). This investigation considered 1079 interproximal areas from 467 periapical radiographs. Experts annotated this data, which was then used to train an Inception and ResNet model that was subsequently tested using a test set. Even with the limited and uneven dataset, Inception produced the best results with an amazing accuracy rate. The results are 0.817, 0.762, 0.923, 0.711, and 0.902 for correspondingly negative predictive values, recall, accuracy, precision, and specificity. The receiver Operating Characteristic (ROC) and Precision-Recall (PR) curves further demonstrate the strong performance of both models. These findings suggest that we can use the assessed CNN model as a clinical decision support tool to diagnose a wrist fracture.

[Meena and Roy \[22\]](#) present a technique for identifying fractures in the seven upper extremity bones (shoulder, humerus, forearm, elbow, wrist, hand, and finger). A proposed two-step classification algorithm is based on the MobileNet model. The first step supplies an improved X-ray image to identify bone type. Based on the first stage's outcome, one of seven classifiers (one for each type of bone) receives the image of the bone to identify its abnormalities. Upon integrating the two phases of classification, an average precision of 73.42% was obtained using the Musculoskeletal Radiographs (MURA) dataset as a performance dataset.

Utilized in numerous applications of medical imaging "for disease diagnosis", according to [Ananthu, et al. \[23\]](#). The scarcity of microscopic pictures for model training, however, is one of the main problems. Transfer learning approaches are proposed as a solution to this problem; researchers compare various transfer learning models, such as MobileNet, to identify Acute Lymphocytic Leukemia (ALL) from blood smear cells. Using the ALL- Interface to the Db2 Database2 dataset, all models were trained, and the MobileNet model yielded an accuracy of 97.88%.

3. METHODOLOGY

The processes in the approach we used for this study include dataset collection, preprocessing, feature extraction, data separation, the suggested deep learning model, training, and testing, as illustrated in [Figure 2](#).

The three main elements of the study's framework are the transfer-learning model, feature engineering, and preprocessing. The authors first performed preprocessing techniques and identified the Return on investment (ROI), then divided the dataset into three sets at ratios of 50%, 12%, and 40% for testing, validation, and training, respectively.

After this, we implemented the data augmentation strategies previously discussed in the data pretreatment section. Preventing the model from overfitting was the primary goal of the dataset augmentation.

The weights of every transfer learning classifier were pre-trained using about 1644 photos from Kaggle. Additionally, we added a single sigmoid function neuron to each pre-trained CNN model's final classification layer, which produces an estimated probability of a given input image being normal or fractured.

Furthermore, we have set the sizes of wrist radiographs to 224×224 for VGG-16 and VGG-19 and 299×299 for Inception V3 and ResNet-50 for each input in order to make them suitable for feeding into every single pre-trained CNN model. The input images used by the RN-22CNN model have a resolution of 150×150 .

The RN-22CNN models link the output layer to its subsequent layers, and their feature classifier layers utilize the data from the immediately preceding layer. Conv 2×2 , 64; conv 2×2 , 128; conv 3×3 , 256, conv 3×3 , 512; 2×2 size of the max-pooling layer; and a softmax activator are the characteristics of the feature selector classifier. The feature selector classifier creates 2-D planes known as feature maps using max-pooling techniques and the final output of the convolution layer.

Once we extract the feature vector from each of these models, we link the output containing the outcome of the last convolutional block to the new feature vector classifier, and freeze the weight of the top convolutional block. The last layer of the model, only utilized by the dense layer, houses the Artificial Neural Network (ANN) feature classifier. This feature classifier, like other classifiers, needs only one vector to finish the computation process.

Consequently as a result, the "flattening" process transforms the output value of the feature vector classifier into a 1-D feature. Sigmoid operations flatten the convolution approach's final output layer, creating a single extended vector that the final dense layer uses in its final classification.

We also positioned the softmax classifier between the activation process and the dense layers to solve the classification problems.

Binary cross-entropy loss was used to compute the loss function. We have also used a grid search to find the ideal hyperparameters, such as learning rate, batch size, etc. Based on the starting rate of learning (e.g., 0.05 and 0.1 models including random selections), a "Stochastic Gradient Descent" (SGD) optimizer with a force of 0.9 was used to adjust each layer of the pre-trained model.

After twenty epochs, there was a 0.1 reduction in the learning rate. The maximum number of epochs that could be executed was 500, and early epoch halting was done to prevent overfitting. We have utilized a batch size of 64 for the RN-22CNN model.

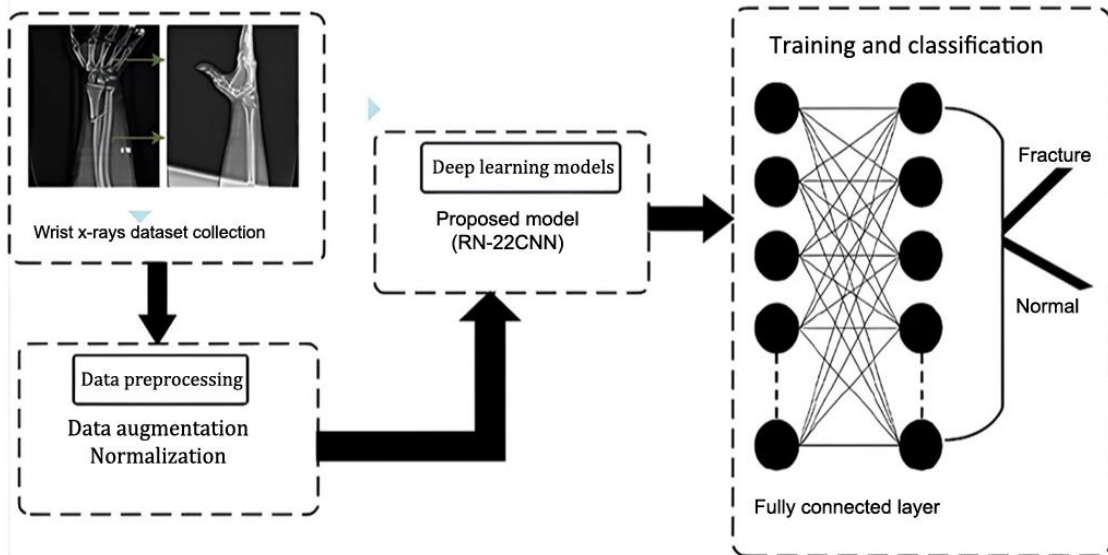


Figure 2. The suggested models for wrist X-ray image fracture detection.

4. DATA COLLECTION

The Kaggle repository is where we took pictures of the bone anomalies. We refer to the dataset as Mura-v1.1. In Mura-v1.1, there are 1644 X-ray pictures of an abnormal wrist. The dataset has been divided into three categories: training, testing, and combined datasets. Splitting ratios are 60% and 40%, respectively, as shown in Figure 3.

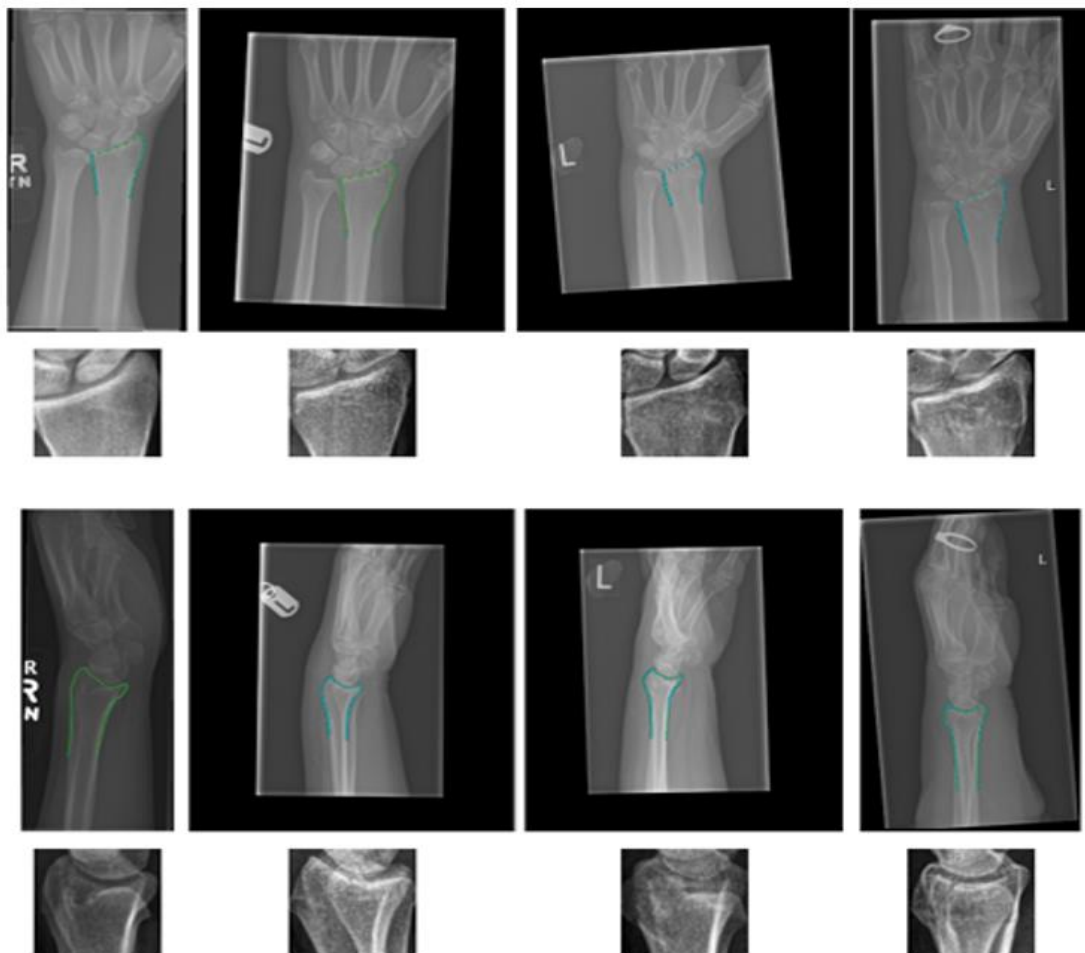


Figure 3. An example of images showing both normal and fractured subjects.

4.1. Data Pre-Processing

Samples of various image sizes are gathered. Thus, photos were resampled to a resolution of 150 x 150. Data standardization was done in order to improve the training process. Since the residual network-based RN22-CNN typically uses a dataset for training, it is set for a fixed size and resolution. We use a variety of data augmentation techniques, including rotation, zoom and width, height shift, lateral and posterior flipping, and scaling, to increase the size of a dataset during training in order to prevent overfitting. After using data augmentation approaches, the model is trained, validated, and tested using a total of 1644 wrist X-ray images, of which 858 are images of fractures and 786 are photos of normalcy.

4.2. Data Augmentation of Wrist X-Ray Images

The amount of data is essential for network training with deep learning-based object detection models. We augmented the data to optimize network training and attain high fracture detection scores. Regarding the original dataset, the Albumentations were used to try a number of augmentation libraries, as shown in Figure 4. A versatile and quick Python library for image augmentation, Albumentations is especially useful for deep learning-based open-source computer vision applications. Examples of these tasks include object recognition, categorization, and segmentation. We carried out augmentations with this library using six distinct techniques: random brightness contrast, sharpness, noise, gamma, gaussian blur, and median blur, either separately or combined. Using them to increase random brightness and contrast has been extremely helpful in identifying breakages within a library of albums.

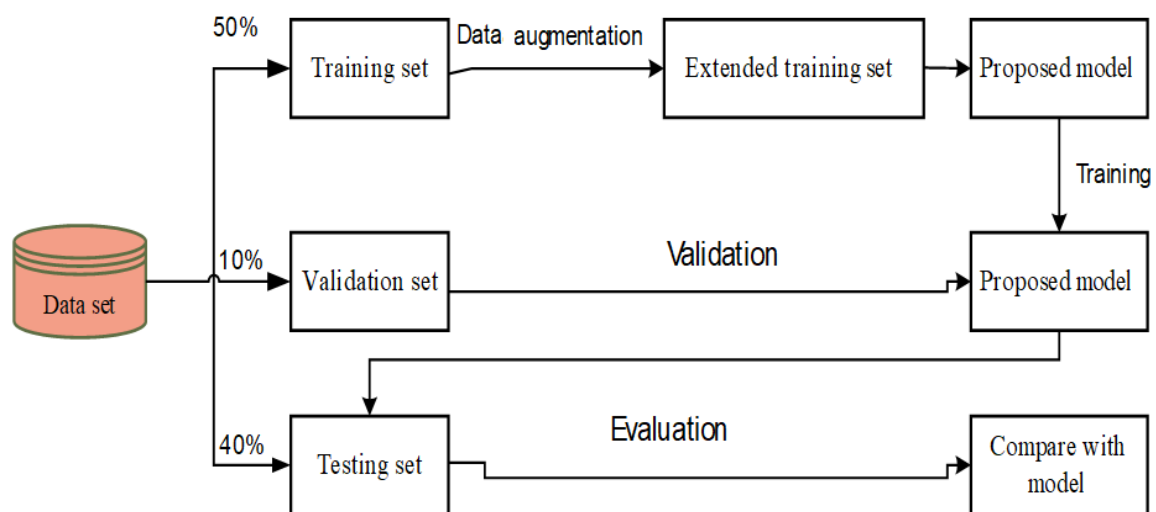


Figure 4. Workflow diagram: Through data augmentation, the number of X-ray pictures is doubled using the expanded training set.

5. FEATURE EXTRACTORS

Research has shown that the selection of the feature extractor can significantly influence the output of the object detection network. The feature extractor's selection is likely critical for casting flaw identification [24]. We decided to use the RN22-CNN architecture as the foundation for our feature extractors. To initialize the feature extractors, we use pertained weights generated from the image dataset. This initialization technique is an example of transfer learning, where the fracture detection and location task uses the information from the image dataset [25].

6. RN-22CNN MODEL

The idea of classifying medical imaging tasks related to wrist fractures was first taken into account to oversee the appropriate creation and design of the RN-22CNN model. X-ray imaging often uses characteristics including target color, spatial connection, form, and texture. Given the fundamental role of a wrist texture feature in

determining wrist type, researchers typically select local features for image description. Despite the fact that texture is a basic and intuitive graphical concept, several research projects have failed to provide a consensus description for the available textures. The architecture of the RN-22CNN model, which is depicted in Figure 5, is our creation. The residual network is the foundation upon which the RN-22CNN model has been constructed. In mathematical statistics, the residual network contains the difference between expected and actual values. Our strategy focuses on learning these small substitutions by highlighting the slight changes and using residual thinking to eliminate similar pieces. According to research, this method fixes the problem where fitting effects deteriorate with the number of neural network layers. 22 layers complicate the process, and after pre-processing, we resize the network's input to a 150 by 150 picture block. Then, we select 1×1 and 3×3 filter sizes for the Convolutional layer.

To get greater non-linear activation, we now utilize the Rectified Linear Unit (ReLU) function with a convolution component smaller than 5×5 and 7×7 . This simplifies the process of training each neuron to accurately record local texture features linked to the desired output, considering the input's accessible field. Even if the previous Convolutional network performed well, the network as a whole was unable to produce precise results in this case. Earlier Convolutional networks simply overlooked some of the data that is strongly connected with the target because of its short size and excessive dimensionality reduction. Consequently, in order to guarantee the preservation of the native network's goal and the reduction of the image's size target, a CNN model based on residual networks is offered by us [26].

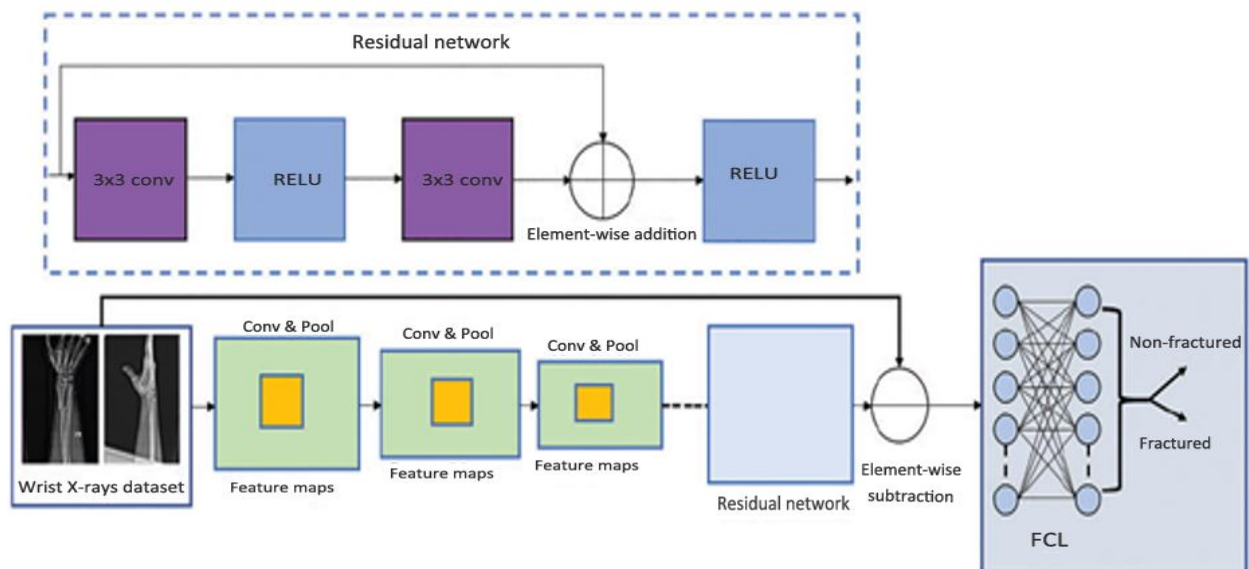


Figure 5. Classifying a patient's wrist fracture using the RN-22CNN design.

Increasing the convolution supports prevents significant harm to the feature map's resolution through an increase in the Convolutional section's receptive area. We introduce a batch normalizing layer after each convolution layer to ensure that the sensitive input area experiences non-linear input value modification and to prevent gradient vanishing concerns brought on by growing training and architectural complexity. The global average pooling layer, which comes after an output from a previous convolution level, finds the average of every feature m . A resultant layer can contain two fully related layers, and its number of feature maps is equal to that of the preceding layer. There are two nodes: the classification layer is the second node, whereas the first layer has 128 nodes. In order to prevent the model from being overfit, we have included a dropout layer with a parameter set to 0.5 before the global pooling layer. When we alter the training procedure, we randomly terminate half of the neurons, and units become dependent on specific inputs [27]. In the neural network model, the activation task is fundamental to the learning and comprehension of a highly complicated and non-linear activity. We understand that the activation function provides neurons with access to non-linear data, enabling a neural network to randomly select any non-linear function. The neural network can also

significantly affect the rate of convergence by choosing the activation function. ReLU prevents gradient vanishing and reduces computing costs compared to standard sigmoid solutions. As a result, the over-fitting issue diminishes, and in most cases, the zero ReLUs of numerous neurons yield notable results, enhancing system sparsity and reducing parameter interdependence. Therefore, the remarkable result of several neurons having zero ReLUs mitigates the over-fitting issue, reducing parameter interdependence and increasing system sparsity. We have employed the ReLU function in this work to activate each of the convolutional layers [28]. A sigmoid compresses the 2D output into a probability distribution for classification, and the first dense layer activates the standard ReLU for the fully linked network layer.

7. PERFORMANCE MEASURES

We evaluated the suggested model's performance using the most commonly used criterion. As seen in Equation 1, by dividing True Positive by the sum of True Positive and False Positive, precision is computed. As shown in Equation 2, recall is determined by dividing the sum of True Positives and False Negatives by the value of True Positives. Two times the Precision times define the F1-score. As in Equation 3, recall is divided by the product of precision and recall [29].

$$P = \frac{\text{True positives}}{\text{True positives} + \text{False positives}} \quad (1)$$

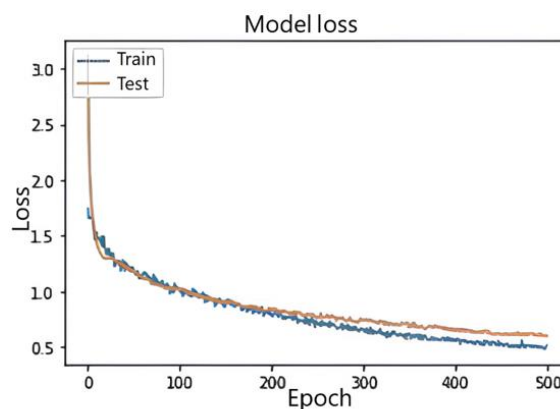
$$R = \frac{\text{True positives}}{\text{True positives} + \text{False negatives}} \quad (2)$$

$$F1 = 2 * \frac{\text{Precision} * \text{Recall}}{\text{precision} + \text{Recall}} \quad (3)$$

8. RESULTS AND DISCUSSION

This section includes the experimental results of the current study, the selected evaluation technique, and the details of the method's implementation. The evaluation techniques for classifying wrist X-ray images rely on a validated and trained test system. Using the test set and training dataset, we trained our model after modifying the hyperparameters for evaluating the RN-22CNN model. Based on the confusion matrix, we have evaluated the model's performance in binary tasks using five metrics: recall, f1-score, accuracy, and accurate overall cataloging computation.

Figure 6 displays the training loss and accuracy validation of the RN-22CNN model for epochs. We ran the CNN model for 500 epochs. The highest possible accuracy for training was 0.99, while the highest possible accuracy for validation was 0.95.



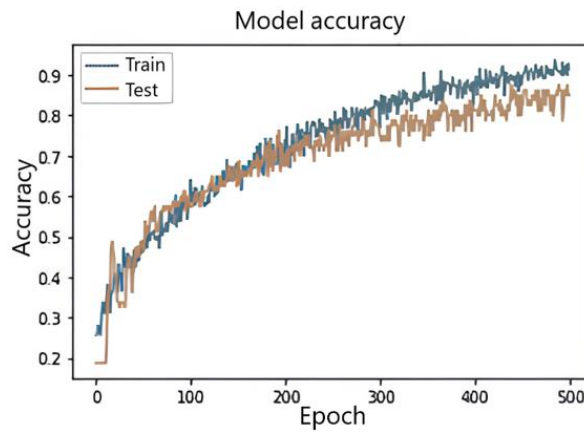


Figure 6. Validating the accuracy and training loss of the RN-22CNN network.

These statistics show that our model learning rate is sound for correctly classifying wrist fractures vs. normal wrists. There was a 0.021 training loss and a 0.026 validation loss. For the purpose of evaluating the model, many performance indicators were examined for the effective diagnosis of wrist fractures. The four pre-trained models and the confusion matrix of the RN-22CNN classifier are shown in Figure 7 and 8, respectively. The test set included 786 photos of normal wrists and 868 photographs of wrist fractures. The confusion matrix arranges actual examples along rows and expected cases along columns.

| | | |
|-----------|-----------------|----|
| The label | 78 | 0 |
| | 1 | 77 |
| | Predicted label | |

Figure 7. Our RN-22CNN model's confusion matrix.

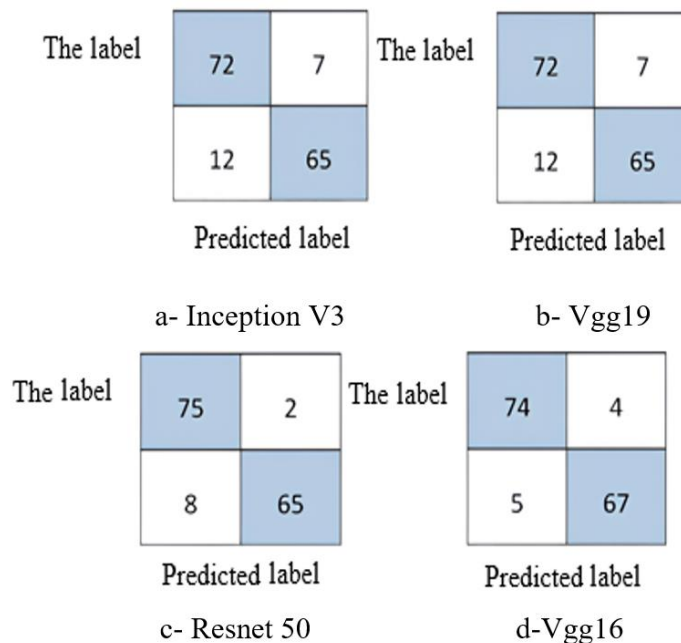


Figure 8. Applications of confusion matrix transfer learning.

Out of 868 wrist fracture instances, the model correctly identified 786 cases for Vgg16, misclassifying 10 cases as normal. Out of 868 wrist fracture cases, the model correctly identified 786 cases as normal, misclassifying 5 of the instances as typical. This is the precise class label for all normal cases predicted by the Vgg19 model. ResNet accurately classified 669 wrist crack instances, misclassifying 200 of the cases as normal. Inception V3 mistakenly classified 180 instances as normal and predicted 665 wrist crack cases. Out of 868 wrist fracture cases, the RN-22CNN model correctly identified 868 of the situations and mistakenly labeled 0 as typical.

The previously mentioned experimental studies show how the RN-22CNN model utilizes the texture feature for precise training of wrist fractures, enabling the identification of the crack region. When compared to other CNN models' classification performance, our method has a 97% accuracy rate for high-quality medical diagnoses in radiography. The Al-Huda digital X-ray laboratory's orthopedic department has appropriately validated the results of the RN-22CNN. Here, we have also covered how well CNN-based pre-trained models work with X-ray images to identify wrist fractures and normal conditions. Pre-trained models like VGG 16, VGG 19, Inception V3, and ResNet 50 & VGG 19 were trained on a moderately small dataset with an image resolution of 224×224 , while the picture resolution is set to 299×299 pixels for Inception V3 and ResNet 50. We trained the RN-21CNN model for wrist fracture classification and all four well-known pre-trained models using a cross-entropy loss function. Imaging with X-rays in this investigation.

Table 1 displays the comparative screening results for each pre-trained model tested. When fine-tuned, the pre-trained VGG 16 model weights showed the best performance, resulting in an accuracy of 77%, a specificity of 68.2%, and a sensitivity of 60.4%. The performance of the transfer learning processes used by the other competitors with pre-trained loads was only slightly worse.

Table 1. RN-22CNN technique comparison using four pre-trained classifiers.

| Technique | Specificity | F1-Score | Sensitivity | Accuracy |
|--------------|-------------|----------|-------------|----------|
| Inception V3 | 80% | 82.2% | 88.4% | 91% |
| Vgg19 | 85% | 70% | 79% | 87% |
| Vgg16 | 68% | 60% | 60% | 77% |
| ResNet 50 | 82% | 79% | 80% | 89% |
| RN-22CNN | 90% | 94% | 92% 99% | 96% |

Additionally, when compared to other transfer learning classifiers, the RN-22CNN model has produced the best classification accuracy, at 96.61%. In general, the choice of pre-trained (CNN) architecture had no effect on the overall binary classification tasks. These networks did not significantly perform better when the number of CNN layers increased for the specific binary diagnostics task. The "Wrist X-ray" dataset provided the 193 X-ray images used in this research study's training. These radiography images were also increased in size for the sake of greater variety and training. These medical images were created at random by applying pixel- and spatial-level image alterations to the X-ray images, such as rotation and scale shifting. One typical criticism of pre-trained models in medical imaging workflows is that they frequently encounter classification issues due to significant target domain divergence. All of the medical images in this dataset had manual labels added by radiologists. By adjusting the model with a limited set of annotated radiograph datasets, we found that transferring information from one domain to another can mitigate the severe consequences of domain deviation. This CNN, using a pre-trained procedure, enables the model to perform and train more quickly, achieving the mutual patterns of both domains. Based on the CNN output, our developed model has a 96.61% diagnostic accuracy when it comes to the categorization of wrist fractures; the RN-22CNN model has outperformed alternative pre-trained CNN-based models. We have elucidated the reasons behind the previous works' inadequate diagnostic performance, together with the analysis of the features of the medical imaging classification task involving wrist fracture, and based on the outputs generated by the different classifiers displayed in Figure 6 and 7. First, deep networks compose the four well-known radiograph classifiers, and the final convolutional layers reduce the

spatial resolution of the feature map, limiting the model's classification accuracy. Additionally, the adjustments made to the algorithms affect the diagnostic performance of the model. These factors include the selection of a suitable learning rate, activation function, loss function, data augmentation techniques, and other essential hyper parameter settings. The RN-22CNN model for categorizing wrist fractures in medical imaging has significantly improved the diagnostic capabilities of medical pictures, as demonstrated by the study of experimental outputs. When it comes to identifying irregularity patterns and distinguishing sequences for categorizing wrist fractures using samples from medical imaging, the RN-22CNN model outperformed other models, achieving a 96.61% accuracy rate. The investigation shows that the RN-22CNN model has significantly improved results when it comes to helping medical professionals locate wrist fracture.

9. CONCLUSION

This work provides a proof-of-concept for analyzing plain medical radiographs using transfer learning from RN22-CNNs pre-trained on real-world images. Despite training the model on a limited sample set, the results matched the state-of-the-art in automated fracture identification. This approach's methodology is very adaptable. There are 22 convolutional layers in this network, and then two dense layers and ReLU activation come next. Dilated convolutions and the Adam optimizer's training process minimize the cross-entropy loss function. The RN-22CNN model technique can avoid the lack of highlight space information while maintaining the model's depth. Given the size of the medical picture data set, this approach has a wide range of potential applications. Using it appropriately can minimize errors, increase workflow productivity, and protect patients by reducing diagnostic delays. Data augmentation enhanced the dataset after gathering it from Kaggle. We separated the dataset into subsets for testing and training. We trained, verified, and examined the updated RN22-CNN model. The suggested mode achieved 96.61 percent accuracy. We intend to keep improving our proposed model's accuracy and time performance in subsequent work. This way, we assist professionals in the timely and effective locational diagnosis of wrist fractures.

Funding: This study received no specific financial support.

Institutional Review Board Statement: Not applicable.

Transparency: The authors state that the manuscript is honest, truthful, and transparent, that no key aspects of the investigation have been omitted, and that any differences from the study as planned have been clarified. This study followed all writing ethics.

Competing Interests: The authors declare that they have no competing interests.

Authors' Contributions: All authors contributed equally to the conception and design of the study. All authors have read and agreed to the published version of the manuscript.

REFERENCES

- [1] B. J. Khadhim, Q. K. Kadhim, W. K. Shams, S. T. Ahmed, and W. W. Alsiadi, "Diagnose COVID-19 by using hybrid CNN-RNN for chest X-ray," *Indonesian Journal of Electrical Engineering and Computer Science*, vol. 29, no. 2, pp. 852-860, 2023. <https://doi.org/10.11591/ijeecs.v29.i2.pp852-860>
- [2] S. M. Naser, Y. H. Ali, and D. A.-J. OBE, "Deep learning model for cyber-attacks detection method in wireless sensor networks," *Periodicals of Engineering and Natural Sciences*, vol. 10, no. 2, pp. 251-259, 2022. <https://doi.org/10.21533/pen.v10i2.2838>
- [3] H. Bisgin *et al.*, "Comparing SVM and ANN based machine learning methods for species identification of food contaminating beetles," *Scientific Reports*, vol. 8, no. 1, p. 6532, 2018. <https://doi.org/10.1038/s41598-018-24926-7>
- [4] M. R. Kumar, K. Pooja, M. Udathu, J. L. Prasanna, and C. Santhosh, "Detection of depression using machine learning algorithms," *International Journal of Online and Biomedical Engineering (iJOE)*, vol. 18, no. 04, pp. 155-163, 2022.
- [5] M. Kumar, D. Shakya, V. Kurup, and W. Suksatan, "COVID-19 prediction through X-ray images using transfer learning-based hybrid deep learning approach," *Materials Today: Proceedings*, vol. 51, pp. 2520-2524, 2022. <https://doi.org/10.1016/j.matpr.2021.12.123>

- [6] S. Candemir and S. Antani, "A review on lung boundary detection in chest X-rays," *International Journal of Computer Assisted Radiology and Surgery*, vol. 14, pp. 563-576, 2019. <https://doi.org/10.1007/s11548-019-01917-1>
- [7] H. A. Mohammed, I. Nazeeh, W. C. Alisawi, Q. K. Kadhim, and S. T. Ahmed, "Anomaly detection in human disease: A hybrid approach using GWO-SVM for gene selection," *Revue d'Intelligence Artificielle*, vol. 37, no. 4, pp. 913-919, 2023. <https://doi.org/10.18280/ria.370411>
- [8] S. Mohanty and M. R. Senapati, "Fracture detection from X-ray images using different machine learning techniques," presented at the 2023 1st International Conference on Circuits, Power and Intelligent Systems (CCPIS). IEEE, 2023.
- [9] A. M. Raisuddin *et al.*, "Critical evaluation of deep neural networks for wrist fracture detection," *Scientific Reports*, vol. 11, no. 1, p. 6006, 2021. <https://doi.org/10.1038/s41598-021-85570-2>
- [10] M. Kraus, R. Anteby, E. Konen, I. Eshed, and E. Klang, "Artificial intelligence for X-ray scaphoid fracture detection: A systematic review and diagnostic test accuracy meta-analysis," *European Radiology*, pp. 1-11, 2023. <https://doi.org/10.1007/s00330-023-10473-x>
- [11] S. T. Ahmed, B. J. Khadhim, and Q. K. Kadhim, "Cloud services and cloud perspectives: A review," in *IOP Conference Series: Materials Science and Engineering*, 2021, vol. 1090, no. 1: IOP Publishing, p. 012078.
- [12] R.-Y. Ju and W. Cai, "Fracture detection in pediatric wrist trauma X-ray images using YOLOv8 algorithm," *Scientific Reports*, vol. 13, no. 1, p. 20077, 2023. <https://doi.org/10.1038/s41598-023-47460-7>
- [13] J. Jabbar, M. Hussain, H. Malik, A. Gani, A. H. Khan, and M. Shiraz, "Deep learning based classification of wrist cracks from X-ray imaging," *Computers, Materials and Continua*, vol. 73, no. 1, pp. 1827-1844, 2022. <https://doi.org/10.32604/cmc.2022.024965>
- [14] F. Uysal, F. Hardalaç, O. Peker, T. Tolunay, and N. Tokgöz, "Classification of shoulder x-ray images with deep learning ensemble models," *Applied Sciences*, vol. 11, no. 6, p. 2723, 2021. <https://doi.org/10.3390/app11062723>
- [15] S. Veronica and J. Sathiaselan, "Classification of long-bone fractures using modified faster RCNN for X-ray," *Indian Journal of Science and Technology*, vol. 16, no. 1, pp. 56-65, 2023. <https://doi.org/10.17485/ijst/v16i1.1690>
- [16] S. T. Ahmed and S. M. Kadhem, "Optimizing Alzheimer's disease prediction using the nomadic people algorithm," *International Journal of Electrical and Computer Engineering*, vol. 13, no. 2, p. 2052, 2023. <https://doi.org/10.11591/ijece.v13i2.pp2052-2067>
- [17] A. M. Barhoom, M. R. J. Al-Hiealy, and S. S. Abu-Naser, "Bone abnormalities detection and classification using deep learning-VGG16 algorithm," *Journal of Theoretical and Applied Information Technology*, vol. 100, no. 20, pp. 6173-6184, 2022. <https://doi.org/10.22214/ijraset.2023.54582>
- [18] A. Esteva *et al.*, "Dermatologist-level classification of skin cancer with deep neural networks," *Nature*, vol. 542, no. 7639, pp. 115-118, 2017. <https://doi.org/10.1038/nature21056>
- [19] C. Cernazanu-Glavan and S. Holban, "Segmentation of bone structure in X-ray images using convolutional neural network," *Advances in Electrical and Computer Engineering*, vol. 13, no. 1, pp. 87-94, 2013. <https://doi.org/10.4316/aece.2013.01015>
- [20] A. Esteva *et al.*, "Deep learning-enabled medical computer vision," *NPJ Digital Medicine*, vol. 4, no. 1, p. 5, 2021. <https://doi.org/10.1038/s41746-020-00376-2>
- [21] M. Moran, M. Faria, G. Giraldo, L. Bastos, and A. Conci, "Do radiographic assessments of periodontal bone loss improve with deep learning methods for enhanced image resolution?," *Sensors*, vol. 21, no. 6, p. 2013, 2021. <https://doi.org/10.3390/s21062013>
- [22] T. Meena and S. Roy, "Bone fracture detection using deep supervised learning from radiological images: A paradigm shift," *Diagnostics*, vol. 12, no. 10, p. 2420, 2022. <https://doi.org/10.3390/diagnostics12102420>
- [23] N. M. M. K. Ananthu, P. K. Chintamaneni, S. B. Shaik, and R. Thadipatri, "Artificial neural networks in optimization of pharmaceutical," *Saudi Journal of Medical and Pharmaceutical Sciences*, vol. 4929, pp. 368-378, 2021.

- [24] S. T. Ahmed and S. M. Kadhem, "Early Alzheimer's disease detection using different techniques based on microarray data: A review," *International Journal of Online & Biomedical Engineering*, vol. 18, no. 4, pp. 106–126, 2022. <https://doi.org/10.3991/ijoe.v18i04.27133>
- [25] E. M. Hameed, I. S. Hussein, H. G. Altameemi, and Q. K. Kadhim, "Liver disease detection and prediction using SVM techniques," presented at the 2022 3rd Information Technology To Enhance e-learning and Other Application (IT-ELA). IEEE, 2022.
- [26] L. Luo *et al.*, "Deep mining external imperfect data for chest X-ray disease screening," *IEEE Transactions on Medical Imaging*, vol. 39, no. 11, pp. 3583–3594, 2020. <https://doi.org/10.1109/tmi.2020.3000949>
- [27] P. Dixit and S. Silakari, "Deep learning algorithms for cybersecurity applications: A technological and status review," *Computer Science Review*, vol. 39, p. 100317, 2021. <https://doi.org/10.1016/j.cosrev.2020.100317>
- [28] M. T. Löffler *et al.*, "A vertebral segmentation dataset with fracture grading," *Radiology: Artificial Intelligence*, vol. 2, no. 4, p. e190138, 2020. <https://doi.org/10.1148/ryai.2020190138>
- [29] Q. K. Kadhim, R. Yusof, H. S. Mahdi, and S. R. Selamat, "The effectiveness of random early detection in data center transmission control protocol - based cloud computing networks," *International Journal on Communications Antenna and Propagation*, vol. 7, pp. 1–7, 2017.

Views and opinions expressed in this article are the views and opinions of the author(s), Review of Computer Engineering Research shall not be responsible or answerable for any loss, damage or liability etc. caused in relation to/arising out of the use of the content.